Supplement to "Comparing efficacies of moxifloxacin, levofloxacin and gatifloxacin in tuberculosis granulomas using a multi-scale systems pharmacology approach"

Elsje Pienaar[1,2], Jansy Sarathy[3], Brendan Prideaux[3], Jillian Dietzold[4], Véronique Dartois[3], Denise E. Kirschner[2] and Jennifer J. Linderman[1]

Pharmacodynamic parameter estimation

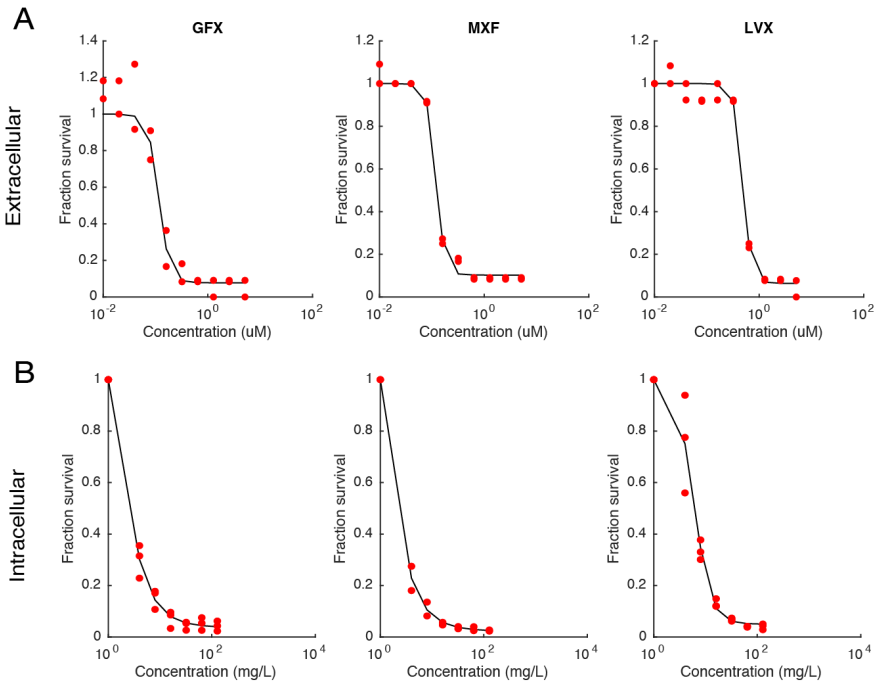

Figure S1: Overlay of in vitro and fitted in silico dose response curves for Mtb in liquid culture after 5 days (A) and in mouse macrophages after 3 days (B). Red data points show in vitro data, and black lines show model fit. X-axis shows antibiotic concentration added in the culture medium.

Fluoroquinolone dynamics in uninvolved rabbit lung samples

There are experimental challenges to isolating truly uninvolved lung tissue in Mtb-infected rabbits. Most lung tissue samples showed some inflammation even in the absence of granulomas. Therefore LCMS measurements in uninvolved lung were not used for calibration of tissue PK parameters. Nonetheless, our in silico predicted concentrations of uninfected simulations are in agreement with measurements in uninvolved (i.e. non-granulomatous) rabbit lung samples (Figure S2). Differences between simulation predictions and rabbit data are most notable for MXF and LVX, and involve earlier peak concentrations predicted in the simulations compared to rabbit data.

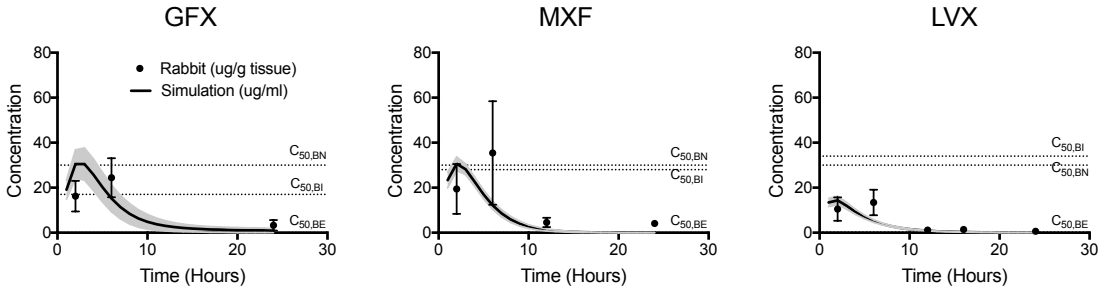

Figure S2: Comparison of average concentrations from simulated uninvolved lung (solid lines) and LCMS measurements in rabbit granulomas (data points). Lines and data points show means and standard deviations for 100 simulations, and between 1 and 67 rabbit samples. Horizontal dashed lines show C_{50} values for intracellular ($C_{50,BI}$), extracellular replicating ($C_{50,BE}$) and extracellular non-replicating bacteria ($C_{50,BN}$).

Spatial fluoroquinolone distribution in granulomas with rabbit and human PK

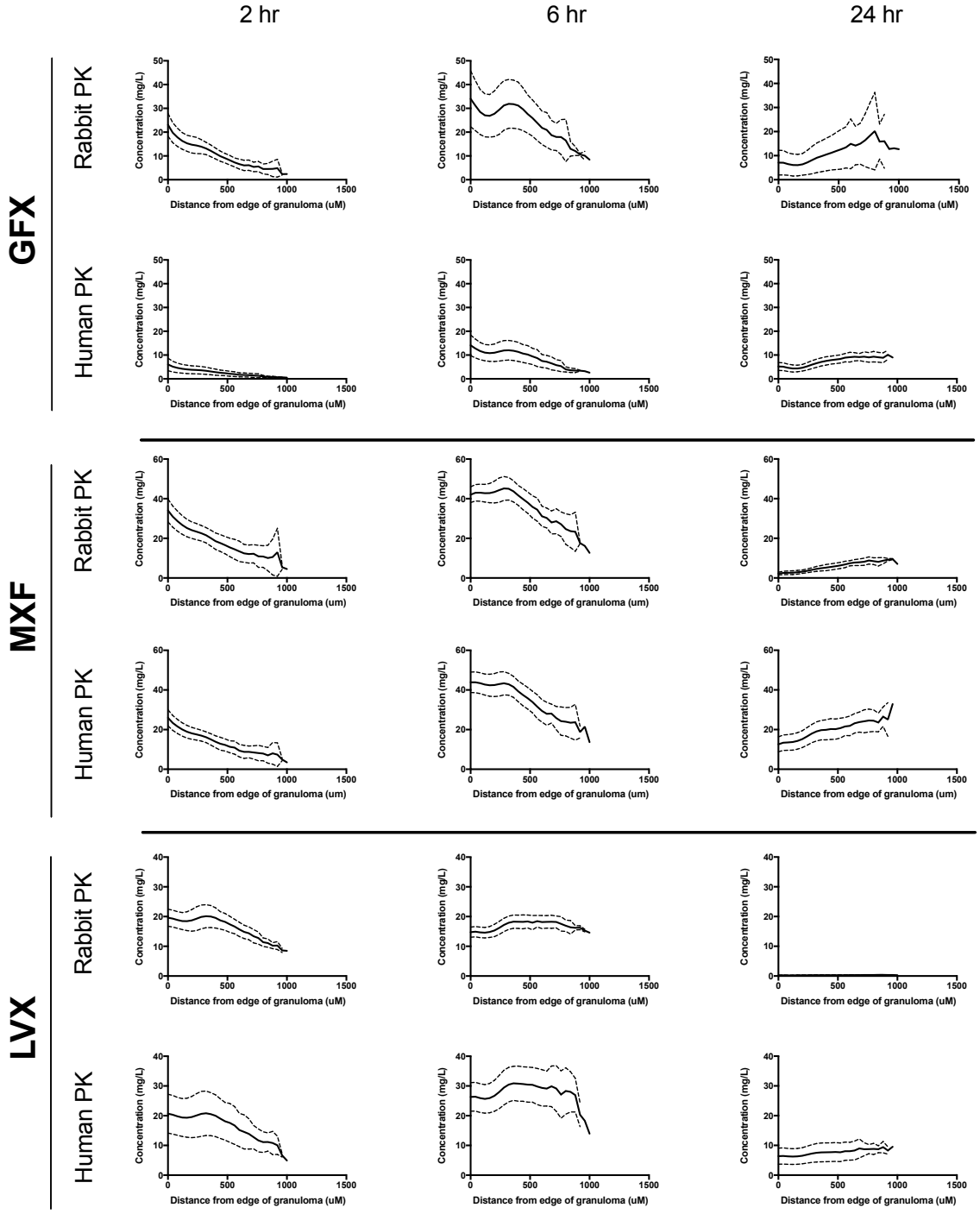

Figure S3: FQ concentrations from simulated granulomas plotted as a function of distance from the edge of the granuloma at 2, 6 and 24 hrs post dose. Solid lines show mean and dashed lines show standard deviation for 100 simulated granulomas.

Bacterial and immune responses following treatment interruption after 70 days

Following treatment interruption after 10 days of treatment (at day 390), bacterial load rebounds more quickly and more steeply for GFX and LVX compared to MXF (Figure 10, main text). However, if treatment is interrupted after 70 days (at day 450) the outcomes are more similar between FQs (Figure S4 A-D). This indicates that bacterial and immunological differences between MXF and the other two FQs that are influential during the first 10 days of treatment, have largely been removed at this later time point (Figure S4 E-F)

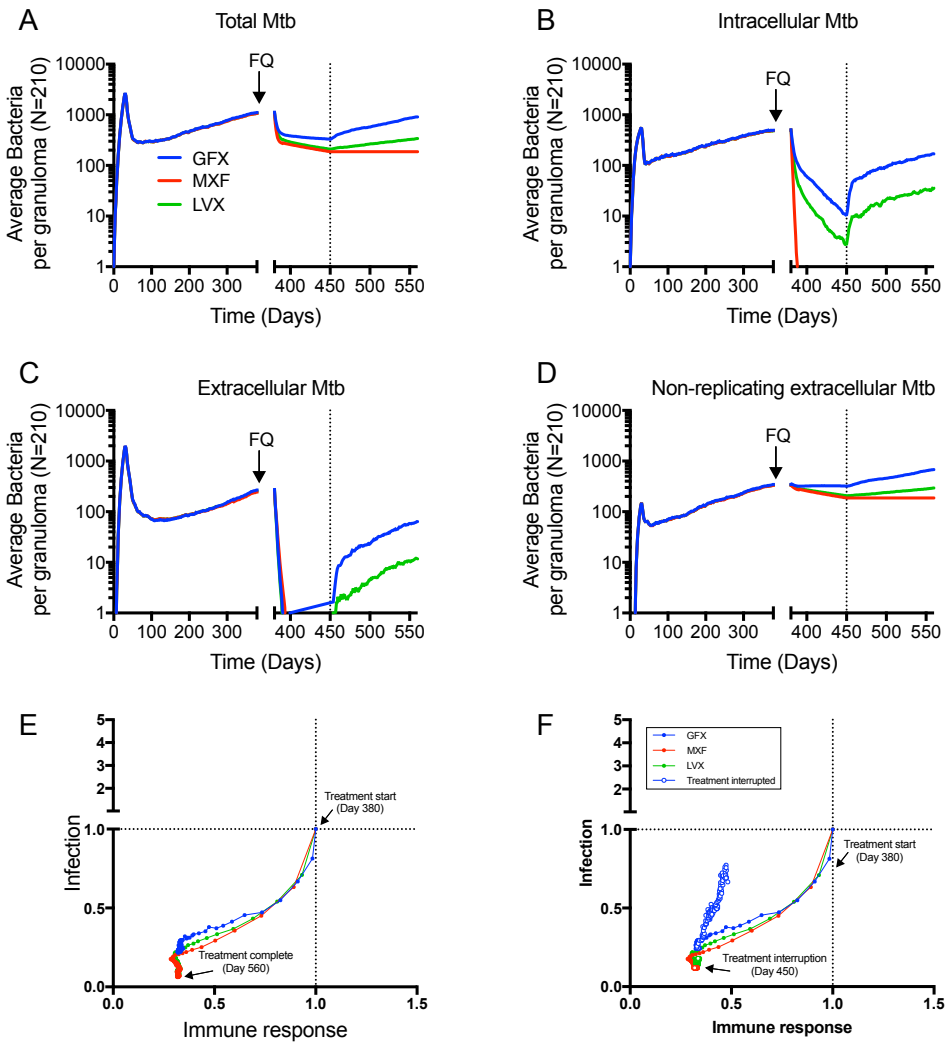

Figure S4: (A-D) Simulations showing intracellular and extracellular bacteria increasing slightly following GFX and LVX interruption, where these populations are eliminated by MXF before day 450. The non-replicating bacterial population shows little change following interruption of any of the FQs. Lines show means of 210 *in silico* granulomas, with infection starting at day 0, daily FQ treatment starting at day 380 (arrows). Treatment is interrupted after 70 days (vertical dotted lines), and the simulation is continued to day 560 without antibiotics. (E-F) Progression of treatment as a function of the collective immune response metric (x-axes) and the collective infection metric (y-axes), during complete treatment (E) and interrupted treatment (F). The start of treatment is located at the intersection of the dotted lines. Filled circles indicate the treatment phase, and open circles indicated progression following treatment interruption.

Host immune parameters varied to capture granuloma variability for tissue PK calibration

Table S1: Host immune parameter ranges used to generate collections of test granulomas to calibrate tissue PK parameters [1,2]

Host Immune Parameters	Unit*	Range (min – max)
Time to heal caseation	Days	8 – 12
TNF threshold for causing apoptosis	Molecules	900 – 1400
Rate of TNF induced apoptosis	s^{-1}	$1.3x10^{-6}$ – $2x10^{-6}$
Minimum chemokine concentration allowing chemotaxis	Molecules	0.4 – 0.6
Maximum chemokine concentration allowing chemotaxis	Molecules	380 – 570
Initial macrophage density	Fraction of grid comp.	0.03 – 0.05
Time steps before a resting macrophage can move	Timesteps	2 – 4
Time steps before an activated macrophage can move	Timesteps	15 – 24
Time steps before an infected macrophage can move	Timesteps	135 – 200
TNF threshold for activating NFkB	Molecules	60 – 90
Rate of TNF induced NFkB activation	s^{-1}	$8x10^{-6}$ – $1.5x10^{-5}$
Probability of resting macrophage killing bacteria		0.1 – 0.15
Adjustment for killing probability of resting macrophages with NFkB activated		0.15 – 0.25
Number of extracellular bacteria in the Moore neighborhood that can activate NFkB	Bacteria	200 – 300
Threshold for intracellular bacteria causing chronically infected macrophages	Bacteria	10 – 15
Threshold for intracellular bacteria causing macrophage to burst	Bacteria	18 – 30
Number of bacteria activated macrophage can phagocytose	Bacteria	4 – 6
Probability of an activated macrophage healing a caseated compartment in its Moore neighborhood		0.004 – 0.007
Number of host cell deaths causing caseation		4 (Caseous granulomas) 15 (Cellular granulomas)
Probability of a T-cell moving to the same compartment as a macrophage		0.035 – 0.055
IFN γ –producing T-cell probability of inducing Fas/FasL mediated apoptosis		0.03 – 0.04
IFN γ –producing T-cell probability of producing TNF		0.04 – 0.05
IFN γ –producing T-cell probability of producing IFN		0.3 – 0.45
Cytotoxic T-cell probability of killing a macrophage		0.007 – 0.01
Cytotoxic T-cell probability of, when it kills a macrophage, also killing all of its intracellular bacteria		0.6 – 0.9
Cytotoxic T-cell probability of producing TNF		0.04 – 0.06
Regulatory T-cell probability of deactivating activated macrophage		0.006 – 0.01
Time before maximum recruitment rates are reached	Timesteps*	790 – 1180
Macrophage maximal recruitment probability		0.25 – 0.4
Macrophage chemokine recruitment threshold	Molecules	0.7 – 1
Macrophage TNF recruitment threshold	Molecules	0.009 – 0.015
Macrophage half sat for TNF recruitment	Molecules	1.3 – 2
Macrophage half sat for chemokine recruitment	Molecules	1.8 – 2.6
IFN γ –producing T-cell maximal recruitment probability		0.12 – 0.18
IFN γ –producing T-cell chemokine recruitment threshold	Molecules	0.0.06 – 0.09
IFN γ –producing T-cell TNF recruitment threshold	Molecules	1 – 1.6
IFN γ –producing T-cell half sat for TNF recruitment	Molecules	1 – 1.6

IFN γ –producing T-cell half sat for chemokine recruitment	Molecules	1.5 – 2.5
Cytotoxic T-cell maximal recruitment probability		0.1 – 0.15
Cytotoxic T-cell chemokine recruitment threshold	Molecules	3.6 – 5.4
Cytotoxic T-cell TNF recruitment threshold	Molecules	1 – 1.5
Cytotoxic T-cell half sat for TNF recruitment	Molecules	1 – 1.5
Cytotoxic T-cell half sat for chemokine recruitment	Molecules	7 – 10
Regulatory T-cell maximal recruitment probability		0.02 – 0.04
Regulatory T-cell chemokine recruitment threshold	Molecules	1.5 – 2.5
Regulatory T-cell TNF recruitment threshold	Molecules	1.3 – 2
Regulatory T-cell half sat for TNF recruitment	Molecules	1.8 – 2.7
Regulatory T-cell half sat for chemokine recruitment	Molecules	1.2 – 1.8

*Conversion factor: 10 min/timestep.

Tissue PK parameter fitting

We estimate tissue PK parameters by calibrating *GranSim* to the in vivo data summarized in Table 2 and Table M2 in the main text. We use Latin Hypercube sampling to sample the parameter space (See Methods). The ranges sampled for each parameter are based on a collection of *in vitro* and literature data (Table S2).

FQ diffusivity ranges in tissue are estimated based on molecular weight, logP and the number of hydrogen donor and acceptor sites based on diffusion studies in tumors [3]. Vascular permeability estimates based on molecular radius alone predict vascular permeability of ~$5x10^{-5}$ cm/s for all three FQs [4]. However, we use vascular permeability ranges one log lower than this estimate ($5x10^{-6}$ cm/s), since we noted that the predicted diffusivity dropped by ~10-fold if one includes the physicochemical properties listed above in addition to the molecular size alone. Furthermore, *in vitro* permeability studies showed that MXF has consistently higher permeability than GFX and LVX by 2- to 10-fold [5]. We estimate initial MXF permeability ranges 2-fold higher than GFX and LVX. Cellular uptake ratio estimates are based on *in vitro* cell uptake assays in THP-1 cells described below. Permeability coefficient estimates are based on plasma protein binding measurements [5]. Caseum unbound fractions are estimated from *in vitro* rapid equilibrium dialysis assays described below.

Table S2: Parameter ranges used for Tissue PK Parameter fitting. The ranges explored during calibration were chosen based on best estimates from experiments and literature for all three FQs. Where no references are given, ranges are based on in vitro data obtained in this work. Final parameter estimates resulting from calibration are given in Table M2 in the main text.

Parameter	Units	MXF		GFX		LVX	
		Experimental/ Literature estimate	Range used in calibration	Experimental/Literature estimate	Range used in calibration	Experimental/Literature estimate	Range used in calibration
Effective diffusivity (D)	cm^2/s	$2.6x10^{-7}$ [3]	$2.6x10^{-8}$ – $2.6x10^{-6}$	$7x10^{-7}$ [3]	$7x10^{-8}$ – $7x10^{-6}$	$4x10^{-7}$ [3]	$4x10^{-8}$ – $4x10^{-6}$
Cellular accumulation ratio [(2)] (a)	-	4.35	0.4 – 40	2.78	0.2 – 20	2.09	0.2 – 20
Vascular permeability (p)	cm/s	$1x10^{-5}$ [4]	$1x10^{-6}$ – $1x10^{-4}$	$5x10^{-6}$ [4]	$5x10^{-7}$ – $5x10^{-5}$	$5x10^{-6}$ [4]	$5x10^{-7}$ – $5x10^{-5}$
Permeability coefficient (PC)	-	0.5 [5]	0.05 – 5	0.8 [5]	0.08 – 8	0.7 [5]	0.07 – 7
Caseum unbound fraction (f_u)	-	0.13	0.05 – 0.3	0.16	0.05 – 0.3	0.18	0.01 – 0.4
Caseum binding rate constant (k_{fc})	$cu^{-1}s^{-1}$		0.0002 – 0.2		0.0002 – 0.2		0.0002 – 0.2
Epithelium binding association constant (K_a)	-		0.01 – 0.02		0.01 – 0.02		0.01 – 0.02
Epithelium binding rate constant (k_{fe})	s^{-1}		0.004 – 0.0099		0.004 – 0.0099		0.004 – 0.0099
Cellular exit rate constant (k_{out})	s^{-1}		0.1 – 0.5		0.1 – 0.5		0.1 – 0.5

Sensitivity analysis

For sensitivity analysis using Partial rank correlations coefficients (PRCC, see Methods), parameters were sampled simultaneously and uniformly in the ranges given in Table S3 using Latin Hypercube sampling (LHS). Significant correlations are summarized in Table S4.

Table S3: Parameters and ranges used in PRCC calculation for sensitivity analysis.

Parameter	Units	Min	Max
Plasma PK parameters [2,3]			
Absorption rate constant (k_a)	h^{-1}	1	10
Intercompartmental clearance rate constant (Q)	L/h/kg	1	10
Plasma volume of distribution (V_p)	L/kg	0.1	1
Peripheral volume of distribution (V_{pe})	L/kg	0.1	1
Plasma clearance rate constant (CL)	L/h/kg	0.1	1
Lung tissue PK parameters [4]			
Effective diffusivity (D)	cm^2/s	$1x10^{-07}$	$1x10^{-06}$
Cellular accumulation ratio [2] (a)	-	1	10
Vascular permeability (p)	cm/s	$1x10^{-06}$	$1x10^{-05}$
Permeability coefficient (PC)	-	1	10
Caseum unbound fraction (f_u)	-	0.1	0.9
Caseum binding rate constant (k_{fc})	$cu^{-1}s^{-1}$	0.005	0.05
Epithelium binding association constant (K_a)	-	0.01	0.03
Epithelium binding rate constant (k_{fe})	s^{-1}	0.002	0.009
Cellular exit rate constant (k_{out})	s^{-1}	0.02	0.2
PD parameters [5]			
Max activity extracellular ($E_{max,BE}$)	s^{-1}	0.001	0.01
Max activity intracellular ($E_{max,BI}$)	s^{-1}	0.001	0.01
C50 for extracellular replicating Mtb ($C_{50,BE}$)	mg/L	0.01	0.1
C50 for extracellular non-replicating Mtb ($C_{50,BN}$) [6]	mg/L	5	50
C50 for intracellular Mtb ($C_{50,BI}$)	mg/L	5	50
Hill constant for intracellular Mtb (H_{BI})	-	1	5
Hill constant for extracellular replicating Mtb (H_{BE})	-	1	5
Hill constant for extracellular non-replicating Mtb (H_{BN})	-	1	5

*Table S4: Significant correlations between model parameters and model outputs. Only significantly correlated parameters are shown. Relationship: '+': positive correlation; '-': negative correlation. Significance: *: $p < 0.01$; **: $p < 0.001$; ***: $p < 0.0001$.*

Significant Parameters

Model outputs	ka	Vp	CL	a	p	PC	Emax,BI	Emax,BE	C50,BN	C50,BI	HBE	fu
Resting macrophages			+++	---		---	---	+		+++		
Infected macrophages			+++	---		---	---			+++		
Chronically infected macrophages			+++	---		---	---			+++		
Activated macrophages			+++	---		---	---			+++		
IFNg producing T cells			+++	---		---	---			+++		
Activated IFNg producing T cells			+++	---		---	---			+++		
Cytotoxic T cells			+++	---		---	---			+++		
Activated cytotoxic T cells			+++	---		---	---			+++		
Regulatory T cells			+++	---		---	---			+++		
Activated regulatory T cells			+++	---		---	---			+++		
Intracellular Mtb			+++	---		---	---			+++		
Extracellular Mtb			+++	---		---	---	---	+++	+++	+++	
Replicating extracellular Mtb		-	+++	---	+++	---	---	---		+++		+
Non-replicating extracellular Mtb			+++	---		---	---	---	+++	+++	+++	
Total MTb			+++	---		---	---	-	+++	+++	+++	
AUC in Blood (0-24hr)	---	+++	---									
AUC in Granuloma (0-24hr)			---	+++		+++		-				---
TNF			+++	---		---	---			+++		
IL10			+++	---		---	---			+++		
Lesion Size			+++	---		---	---			+++		
Caseation level			+++	---		---	---			+++		

References

1 Pienaar, E. *et al*. A computational tool integrating host immunity with antibiotic dynamics to study tuberculosis treatment. *J Theor Biol* **367**, 166-179, doi:10.1016/j.jtbi.2014.11.021 (2015).

2 Pienaar, E., Dartois, V., Linderman, J. J. & Kirschner, D. In silico evaluation and exploration of antibiotic tuberculosis treatment regimens. *BMC systems biology* **9**, 79, doi:10.1186/s12918-015-0221-8 (2015).

3 Pruijn, F. B., Patel, K., Hay, M. P., Wilson, W. R. & Hicks, K. O. Prediction of Tumour Tissue Diffusion Coefficients of Hypoxia-Activated Prodrugs from Physicochemical Parameters. *Australian Journal of Chemistry* **61**, 687-693 (2008).

4 Schmidt, M. M. & Wittrup, K. D. A modeling analysis of the effects of molecular size and binding affinity on tumor targeting. *Molecular cancer therapeutics* **8**, 2861-2871, doi:10.1158/1535-7163.MCT-09-0195 (2009).

5 Lakshminarayana, S. B. *et al*. Comprehensive physicochemical, pharmacokinetic and activity profiling of anti-TB agents. *The Journal of antimicrobial chemotherapy* **70**, 857-867, doi:10.1093/jac/dku457 (2015).